

# ЛМФ 2013 (Гамма-нуклон)

## Лаборатория мезонной физики ОФВЭ

Отчет о ходе выполнения научно-исследовательской  
работы

«Барионная спектроскопия и физика с  $\eta$ -мезонами.»

1. Бонн, CB-ELSA
2. Бонн, BGO-OD
3. Майнц, CB+TAPS

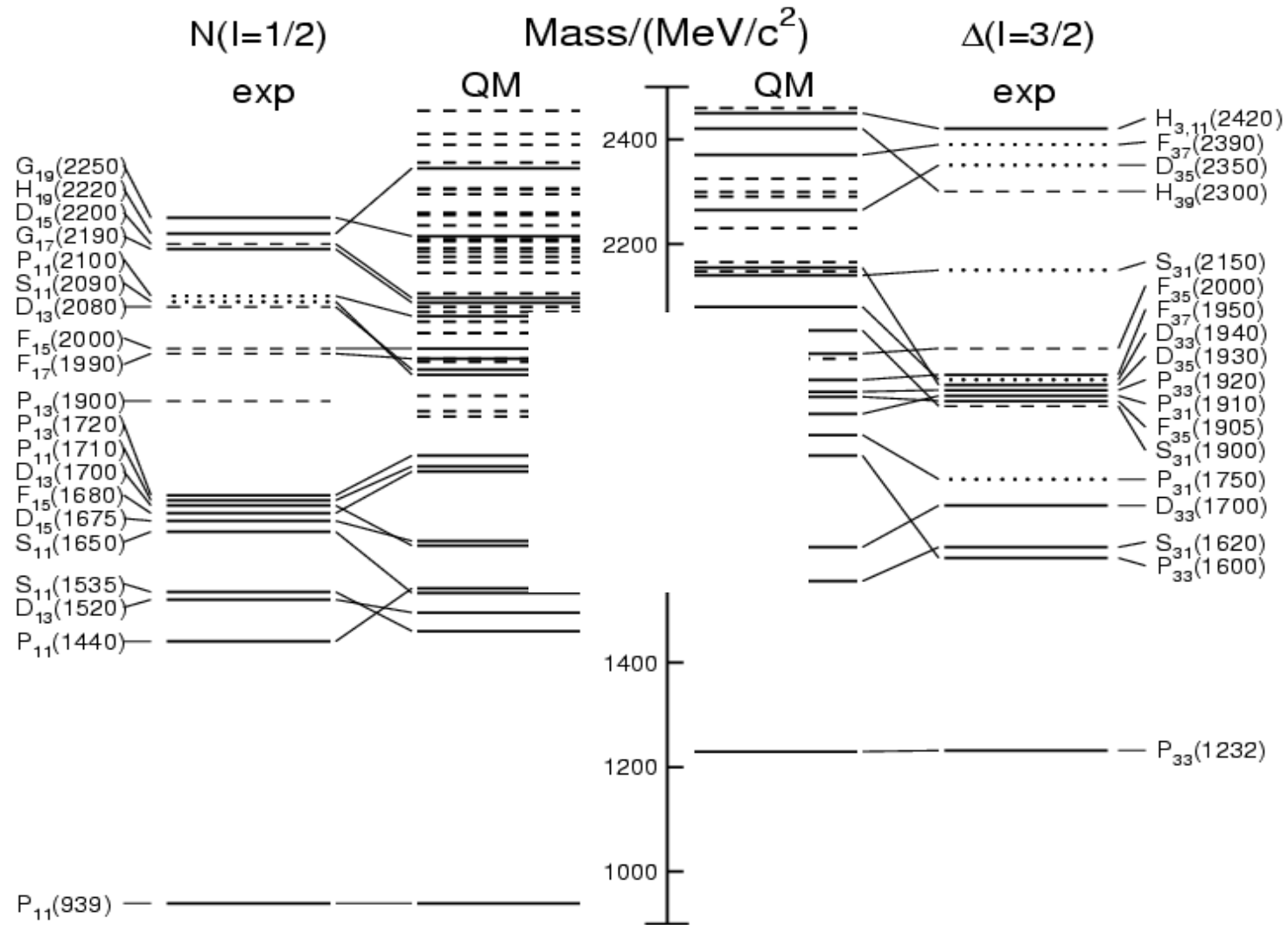
2013 г.

Отчёт составил зав. ЛМФ В.В.Сумачёв.

## Сравнение результатов анализов и предсказаний моделей для числа $N^*$ and $\Delta$ -резонансов.

References	$N^*$ – resonance number	$\Delta$ – resonance number
Rev. of Part. Phys. (1980)	26	19
Rev. of Part. Phys. (2010)	23	22
KH80	21	18
KA84	18	16
CMB (Phys.Rev.D 20 1979 )	16	13
T.P.Vrana et al.( nucl-th/9910012 )	14	13
SM95 (Phys.Rev.C 52 1995 )	13	8
FA02 ( Phys.Rev.C 69, 2004 )	10	7
SP06 ( nucl-th/0605082 )	13	9
S.Capstick et al.(Phys.Rev.D 49,1994)	40	27
U.Loring et al.(hep-ph/0103289)	99	82
Skyrme model (Phys.Rev.D31,1985)	10	13
J.Vijande et al.( hep-ph/0312165 )	19	21

In the PDG 2010 Baryon summary table there are in general ( $N^*$ ,  $\Delta$ ,  $\Lambda$ ,  $\Sigma$  and others) 131 baryon.  $n=4$ , three 70-plets and four 56-plets are given in summary tables. In general 434 baryons must be.



## Экспериментальные данные по спиновой физике в гамма-протон взаимодействии на установке CB-ELSA (Бонн)

Участники от Лаборатории мезонной физики:

Д.Е. Баядилов, Ю.А. Белоглазов, А.Б. Гриднев, И.В. Лопатин,  
Д.В. Новинский, А.К. Радьков, В.В. Сумачёв.

## Ускоритель - ELectron Stretcher Anlage (ELSA)

- Energy range 0.5–3.5 GeV
- Max. extracted intensity  $\sim 1\text{nA}$
- Electron polarisation  $\sim 60\text{--}80\%$

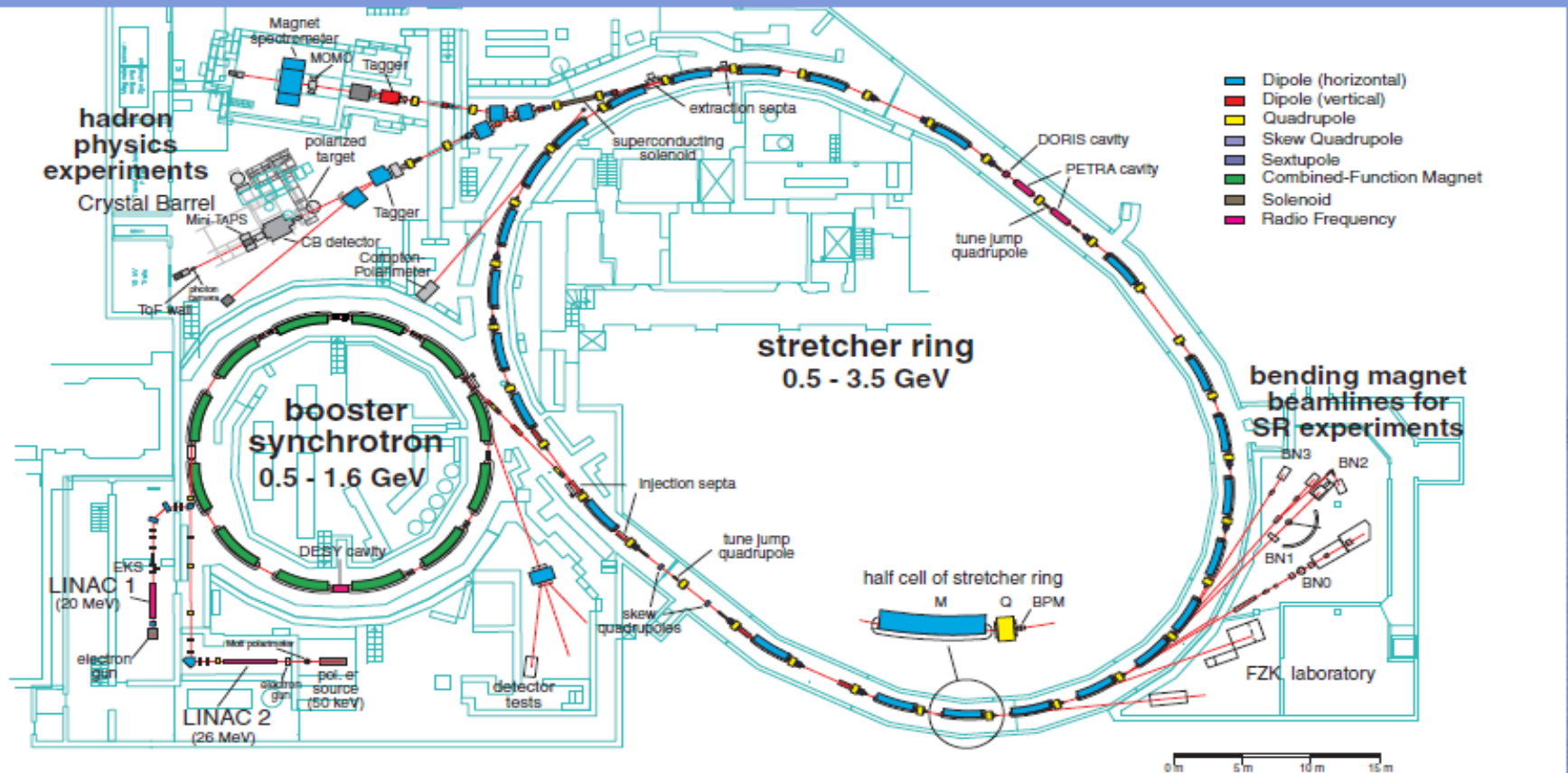
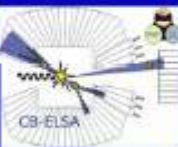
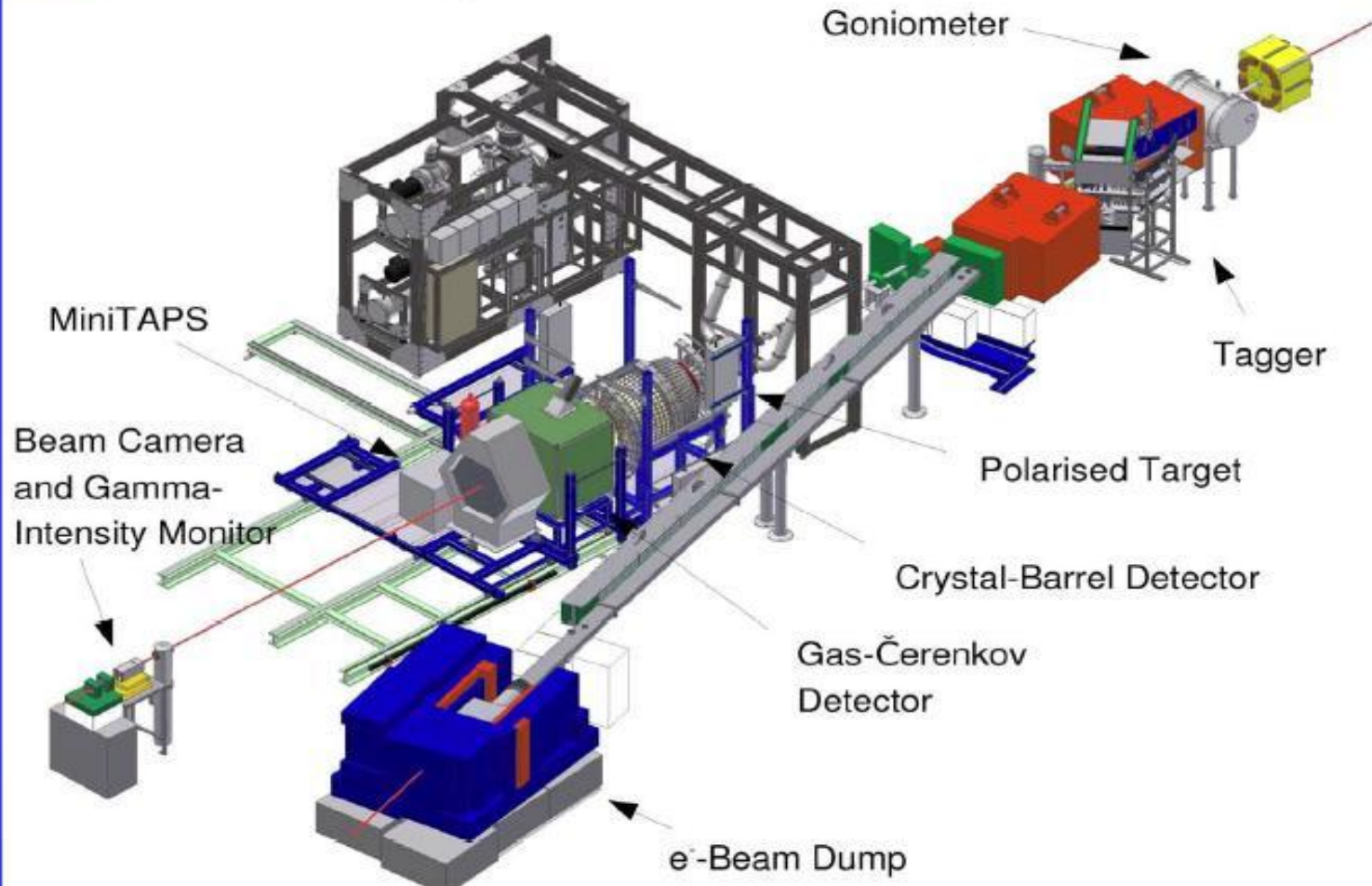


Схема установки CB-ELSA

universität**bonn**

# The Crystal-Barrel Experiment



Photon		Target	Recoil	Target-Recoil
		$x \quad y \quad z$	$x' \quad y' \quad z'$	$x' \quad x' \quad z' \quad z'$ $x \quad z \quad x \quad z$
unpolarized	$\sigma$	$0 \quad T \quad 0$	$0 \quad P \quad 0$	$T_{x'} \quad -L_{x'} \quad T_{z'} \quad L_{z'}$
linearly	$-\Sigma$	$H \quad (-P) \quad -G$	$O_{x'} \quad (-T) \quad O_{z'}$	$(-L_{z'}) \quad (T_{z'}) \quad (-L_{x'}) \quad (-T_{x'})$
circularly	$0$	$F \quad 0 \quad -E$	$C_{x'} \quad 0 \quad C_{z'}$	$0 \quad 0 \quad 0 \quad 0$

- the 4 independent helicity amplitudes of single pseudoscalar meson photoproduction can be uniquely determined by 8 out of 16 accessible observables, among:
  - 4 double polarization observables (at least 2 recoil observables),
  - 2 with transversally polarized target,
- with transversally polarized target, P can be measured without measuring the polarization of the recoil proton
- complete set:  $\Sigma, \sigma, T, P, G, E, C_{x'}, C_z$
- $C_{x'}, C_z$  are measured for single  $\pi$  production (Phy. Rev. C66 034614 2002)
  - with these measurements a complete experiment is possible

## Determination of the $\eta'$ -nucleus optical potential

### Abstract

The excitation function and momentum distribution of  $\eta'$  mesons have been measured in photon induced reactions on  $^{12}\text{C}$  in the energy range of 1250-2600 MeV. The experiment was performed with tagged photon beams from the ELSA electron accelerator using the Crystal Barrel and TAPS detectors. The data are compared to model calculations to extract information on the sign and magnitude of the real part of the  $\eta'$ -nucleus potential. Within the model, the comparison indicates an attractive potential of  $-(37 \pm 10(\text{stat}) \pm 10(\text{syst}))$  MeV depth at normal nuclear matter density. Since the modulus of this depth is larger than the modulus of the imaginary part of the  $\eta'$ -nucleus potential of  $-(10 \pm 2.5)$  MeV, determined by transparency ratio measurements, a search for resolved  $\eta'$ -bound states appears promising.

(Dated: November 4, 2013)



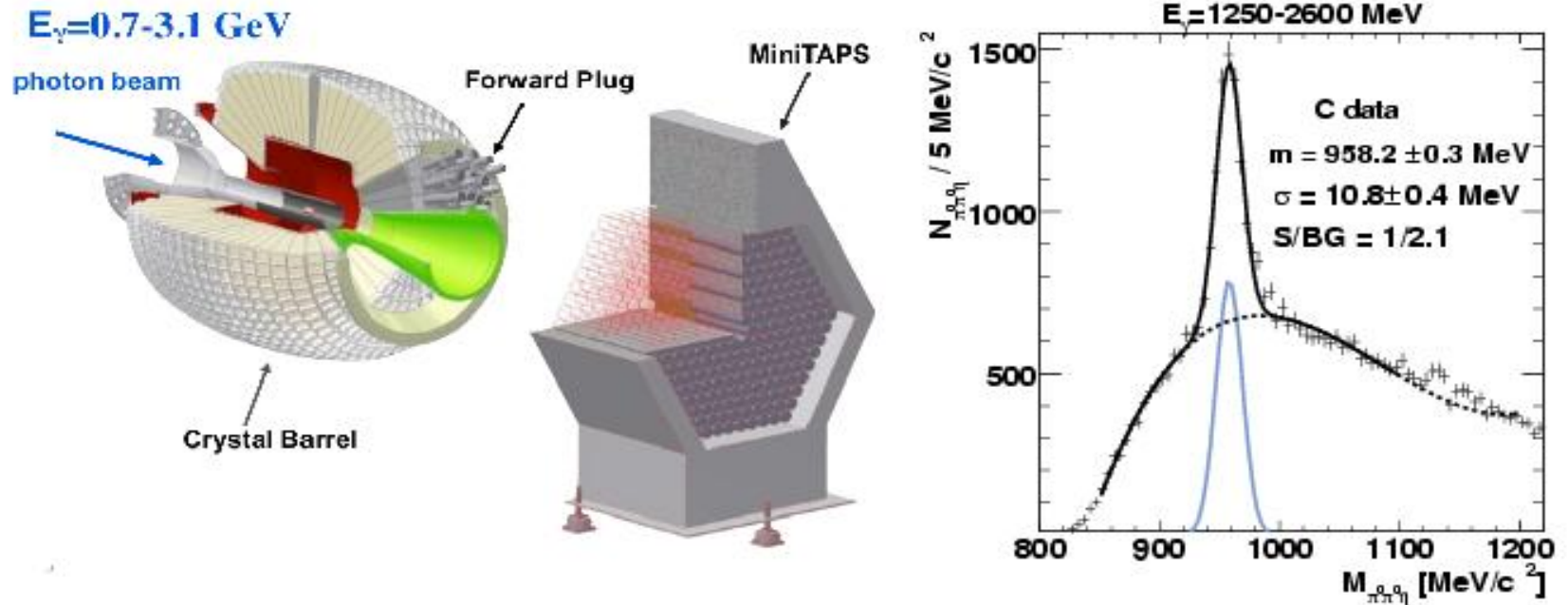


FIG. 1. (Color online) Left: Setup used in the experiment in 2009. Right: The  $\pi^0\pi^0\eta$  invariant mass distribution measured in photoproduction off carbon in the incident photon energy range of 1250-2600 MeV. The solid curve represents a fit to the data using a Gaussian function combined with a polynomial function for the background. The fit parameters are:  $\sigma=10.8\pm 0.4$  MeV (corresponding to the instrumental resolution),  $m=958.2\pm 0.3$  MeV/ $c^2$ ; S/BG is the signal (S) to background (BG) ratio within a  $\pm 3\sigma$  interval.

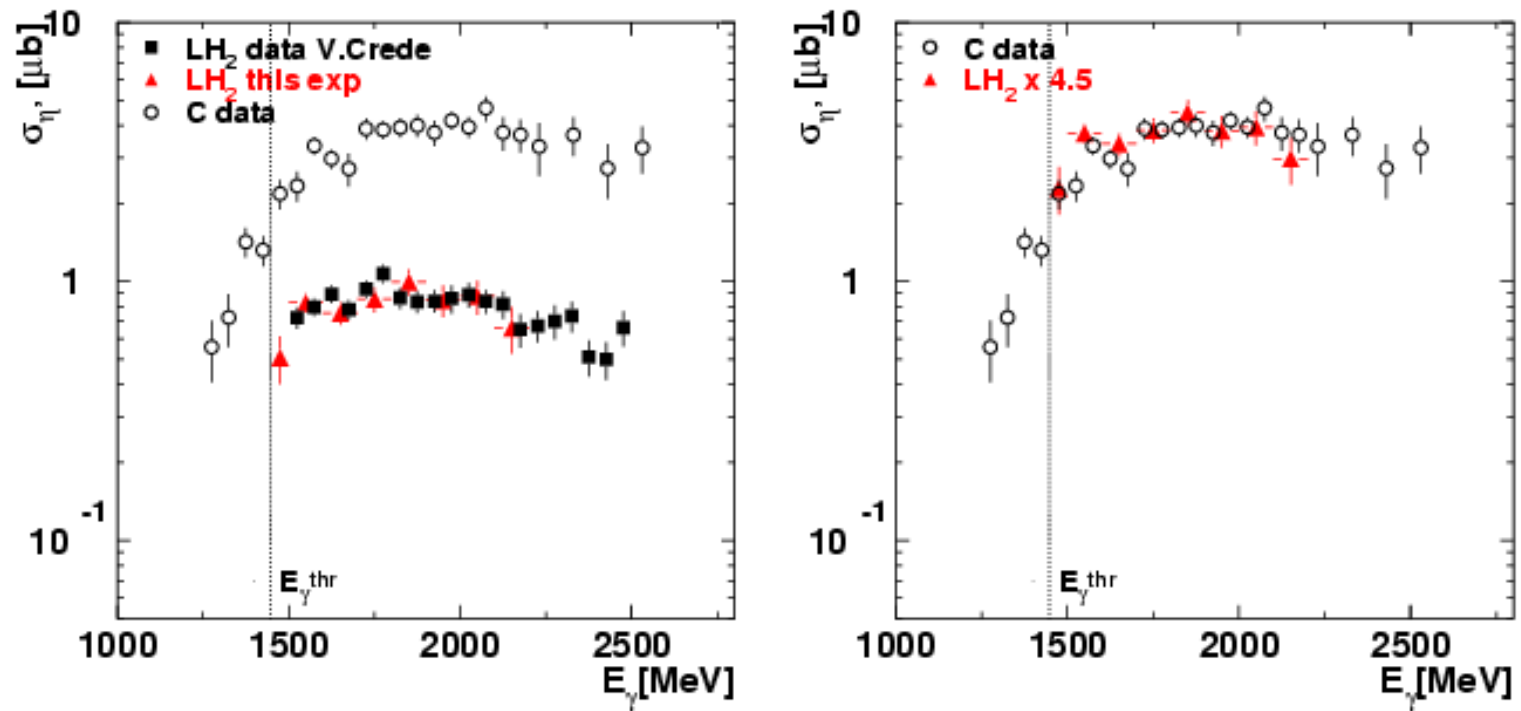


FIG. 3. (Color online) Left: Total cross sections for  $\eta'$  photoproduction off C (open points), in comparison to those for  $\eta'$  production off the proton from this experiment (triangles) and from [26] (full squares). Right: Total cross section for  $\eta'$  production off the proton from this experiment scaled up by factor of 4.5 to match the cross section for  $\eta'$  production off C.

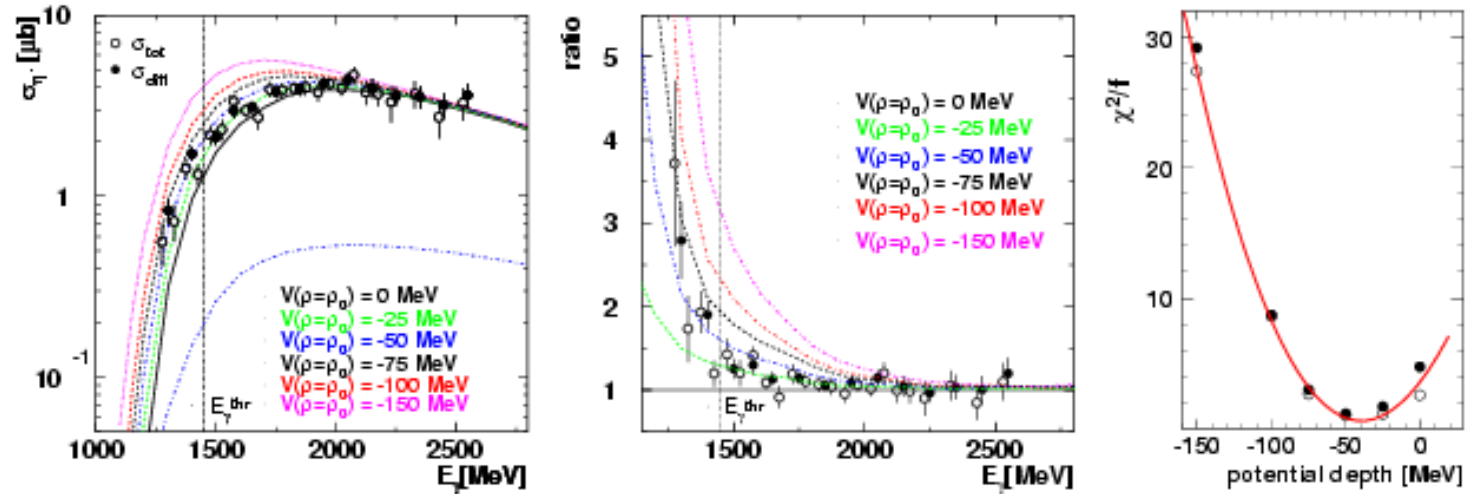


FIG. 4. (Color online) Left: Total cross section for  $\eta'$  photoproduction off C. The experimental data are extracted by integrating the differential cross sections (full circles) and by direct measurement of the  $\eta'$  yield in the incident photon energy bins of width  $\Delta E_\gamma=50$  MeV (open circles). The calculations are for  $\sigma_{\eta'N}=11$  mb and for potential depths  $V=0$  MeV (black line), -25 MeV (green), -50 MeV (blue), -75 MeV (black dashed), -100 MeV (red) and -150 MeV (magenta) at normal nuclear density, respectively, and using the full nucleon spectral function. The dot-dashed blue curve is calculated for correlated intranuclear nucleons only (high-momentum nucleon contribution). All calculated cross sections have been reduced by a factor 0.75 (see text). Middle: The experimental data and the predicted curves for  $V=-25, -50, -75, -100$  and -150 MeV divided by the calculation for scenario of  $V=0$  MeV and presented on a linear scale. Right:  $\chi^2$ -fit of the data with the calculated excitation functions for the different scenarios over the full incident photon energy range.

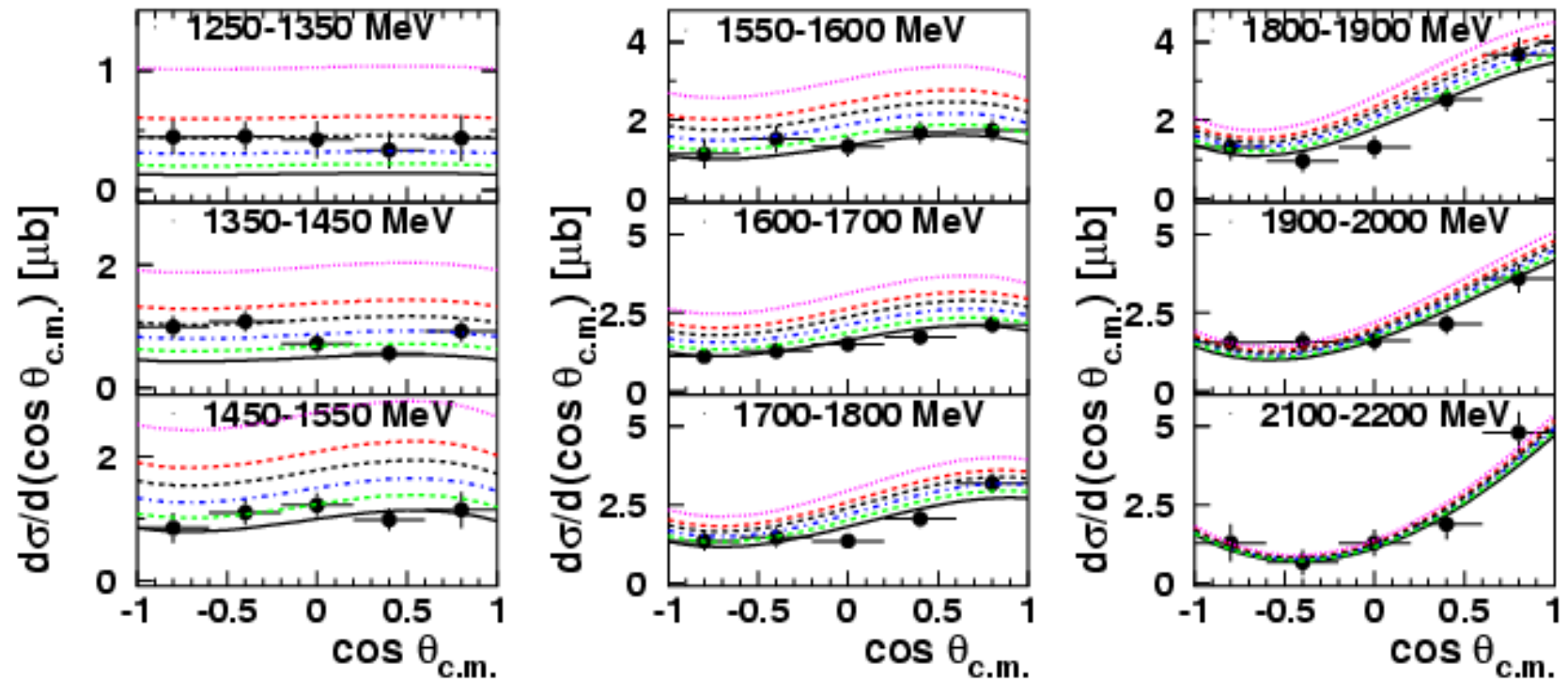


FIG. 5. (Color online) Differential cross sections for  $\eta'$  photoproduction off C for incident photon energies below the free production threshold (left), at the threshold (middle), and above the threshold (right). The calculations are for  $\sigma_{\eta'N}=11$  mb and for potential depths  $V=0, -25, -50, -75, -100$  and  $-150$  MeV, at normal nuclear density, respectively. All calculated cross sections have been reduced by a factor 0.75 (see text). The colour code is identical to the one in Fig.4.

## Determination of the $\eta'$ -nucleus optical potential

### VI. CONCLUSIONS

Experimental approaches to determine the  $\eta'$ -nucleus optical potential have been presented and discussed. The imaginary part of the  $\eta'$ -nucleus optical potential, deduced from transparency ratio measurements, has been found to be  $(-10 \pm 2.5)$  MeV [11]. Within the model used, the present results on the real part of the potential are consistent with an attractive  $\eta'$ -nucleus potential with a depth of  $-(37 \pm 10(\text{stat}) \pm 10(\text{syst}))$  MeV. This result implies the first (indirect) observation of a mass reduction of a pseudo-scalar meson in a strongly interacting environment under normal conditions ( $\rho = \rho_0, T = 0$ ). The attractive  $\eta'$ -nucleus potential might even be strong enough to allow the formation of bound  $\eta'$ -nucleus states. The search for such states is encouraged by the relatively small in-medium width of the  $\eta'$  [11]. Experiments are proposed to search for  $\eta'$  bound states via missing mass spectroscopy [35] at the Fragment Separator (FRS) at GSI and in a semi-exclusive measurement at the BGO-Open Dipol (OD) setup at the ELSA accelerator in Bonn [36], where observing the formation of the  $\eta'$ -mesic state via missing mass spectroscopy will be combined with the detection of its decay. A corresponding semi-exclusive experiment is also proposed for the Super-FRS at FAIR [37]. The observation of  $\eta'$ -nucleus bound states would provide further direct information on the in-medium properties of the  $\eta'$  meson.

## First measurement of the helicity asymmetry for $\gamma p \rightarrow p\pi^0$ in the resonance region

(The CBELSA/TAPS Collaboration)

<sup>1</sup>*Helmholtz-Institut für Strahlen- und Kernphysik, Universität Bonn, Germany*

<sup>2</sup>*Physikalisches Institut, Universität Bonn, Germany*

<sup>3</sup>*II. Physikalisches Institut, Universität Gießen, Germany*

<sup>4</sup>*Physikalisches Institut, Universität Basel, Switzerland*

<sup>5</sup>*Petersburg Nuclear Physics Institute, Gatchina, Russia*

<sup>6</sup>*Institut für Experimentalphysik I, Ruhr-Universität Bochum, Germany*

<sup>7</sup>*Department of Physics, Florida State University, Tallahassee, FL 32306, USA*

(Dated: October 21, 2013)

The first measurement of the helicity dependence of the photoproduction cross section of single neutral pions off protons is reported for photon energies from 600 to 2300 MeV, covering nearly the full solid angle. The data are compared to predictions from the SAID, MAID, and E<sub>0</sub>G<sub>0</sub> partial wave analyses. Strikingly large differences between data and predictions are observed which are traced to differences in the helicity amplitudes of well known and established resonances. Precise values for the helicity amplitudes of several resonances are reported.

$$\frac{d\sigma}{d\Omega} = \frac{d\sigma_0}{d\Omega} (1 \pm P_T P_\odot E). \quad (3)$$

When a butanol ( $C_4H_9OH$ ) target is used, unpolarized ( $u$ ) free protons ( $f$ ) as well as nucleons bound ( $b$ ) in carbon or oxygen contribute to the count rate, in addition to the polarized ( $p$ ) free protons. For the same number of beam photons for both photon helicities, and under the assumption that (unpolarized) nucleons bound in carbon have the same response to impinging photons as nucleons bound in oxygen, we get for beam and target polarized in the same direction the yield  $N_{3/2} = N_{3/2}^{f,p} + N^{f,u} + N^b$  and in opposite direction  $N_{1/2} = N_{1/2}^{f,p} + N^{f,u} + N^b$ , which leads to

$$E = \frac{N_{1/2} - N_{3/2}}{N_{1/2} + N_{3/2}} \cdot \frac{1}{d} \cdot \frac{1}{P_\odot P_T}. \quad (4)$$

The bound nucleons are taken into account by the dilution factor  $d = \frac{N^f}{N^f + N^b}$ . It was determined by an additional measurement using a carbon foam target with approximately the same density, size, and environment as the carbon and oxygen part of the butanol target.

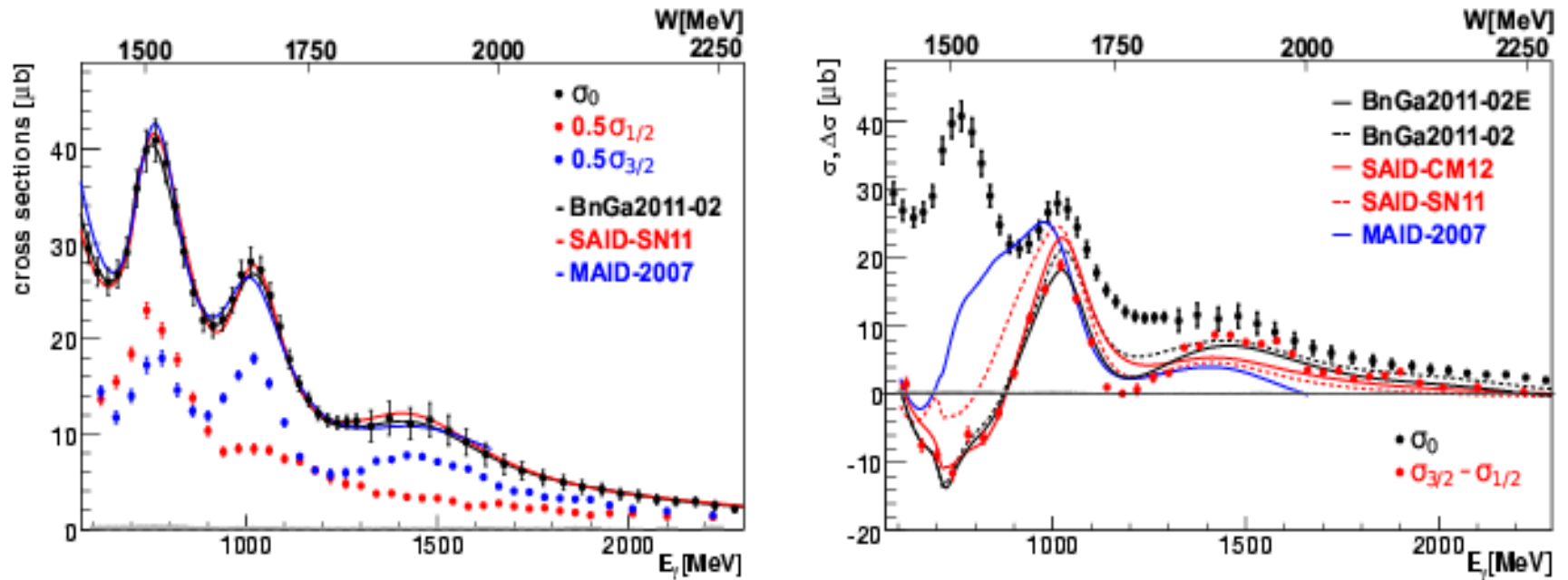


Figure 1: The total cross section  $\sigma_0$  [28] plotted together with its two helicity components (left) and  $\sigma_{3/2} - \sigma_{1/2}$  (right) as a function of  $E_\gamma$ . The error bars give the statistical errors, the systematic errors are shown as a dark gray band.



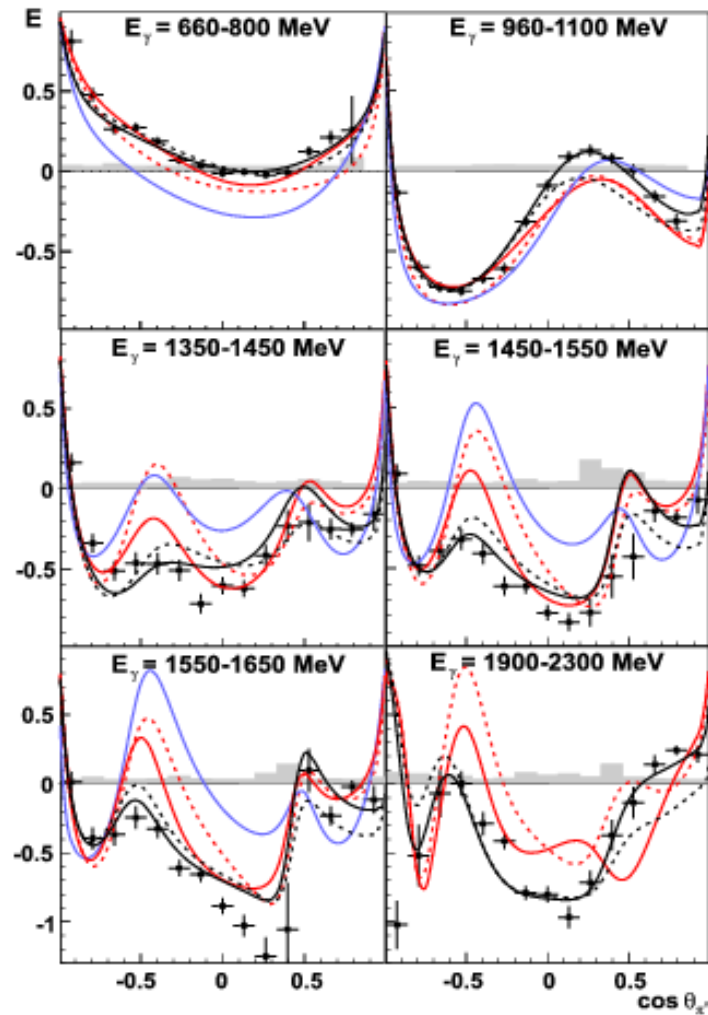


Figure 2: The helicity asymmetry  $E$  as a function of  $\cos \theta_\pi$  for selected  $E_\gamma$  bins. PWA predictions: black dashed curve: BnGa2011-02, blue solid curve: MAID, red solid curve: CM12, red dashed curve: SN11. Fit to the data points (BnGa2011-02E): black solid curve.

	MAID2007	SN11	CM12	BnGa2011	BnGa2011E		MAID2007	SN11	CM12	BnGa2011	BnGa2011E
N(1440)						N(1520)					
M	1440	1485	1485	1430±8	1430±8		1530	1515	1515±3	1517±3	1516±2
Γ	350	284	284	365±35	360±30		130	104	104±5	114±5	113±5
BR(Nπ)	70	79	79	62±3	62±3		60	63	63±3	62±3	62±2
A <sub>1/2</sub>	-61	-58±1	-56±1	-61±6	-62±8		-27	-16±2	-19±2	-22±4	-20±3
A <sub>3/2</sub>							161	156±2	141±2	131±10	131±7
N(1535)						N(1650)					
M	1535	1547	1547	1519±5	1518±4		1690	1635	1635	1651±6	1651±6
Γ	100	188	188	128±14	125±10		100	115	115	104±10	102±10
BR(Nπ)	40	36	36	54±5	55±5		85	100	100	51±4	50±4
A <sub>1/2</sub>	66	99±2	128±4	105±10	105±9		33	65±25	55±30	33±7	33±7
Δ(1620)						Δ(1950)					
M	1620	1615	1615	1600±8	1598±6		1945	1921	1921	1915±6	1915±5
Γ	150	147	147	130±11	130±8		280	271	271	246±10	249±8
BR(Nπ)	25	32	32	28±3	28±3		40	47	47	45±2	46±2
A <sub>1/2</sub>	66	64±2	29±3	52±5	52±5		-94	-71±2	-83±4	-71±4	-70±5
A <sub>3/2</sub>							-121	-92±2	-96±4	-94±5	-93±5

Table I: Properties of selected low-mass nucleon resonances. Breit-Wigner mass, width, and  $N\pi$  partial decay width as defined in [9] are given in MeV, the helicity amplitudes in  $10^{-3} \text{ GeV}^{-1/2}$ .

First measurement of the helicity asymmetry for  $\gamma p \rightarrow p\pi^0$  in the resonance region

Summarizing, we have reported the first measurement of the helicity dependent photoproduction cross section for photons at  $E_\gamma = 0.6\text{-}2.3$  GeV with nearly full solid angular coverage. The observable  $E$  is shown to be highly sensitive to the contributions from  $s$ -channel resonances. Even after many years of studying the simplest photoproduction reaction,  $\gamma p \rightarrow p\pi^0$ , the new data reveal very significant discrepancies in comparison with model predictions. As expected, it is obvious that a fit to differential cross sections and to single polarization observables alone is not sufficient to arrive at unambiguous solutions.

## Recent Results of the BGO-OD Experiment at ELSA Facility

### BGO-OD-Kollaboration

TINA BANTES<sup>1</sup>, DAIR BAYADILOV<sup>2</sup>, REINHARD BECK<sup>2</sup>, MAX BECKER<sup>2</sup>, ANDREAS BELLA<sup>1</sup>, JOHN BIELING<sup>1</sup>, SABINE BOESE<sup>2</sup>, ALESSANDRO BRAGHIERI<sup>3</sup>, KAI BRINKMANN<sup>2</sup>, DMYTRO BURDEYNYT<sup>4</sup>, GORDON DIEFENTHAL<sup>2</sup>, RACHELE DI SALVO<sup>5</sup>, HARTMUT DUTZ<sup>1</sup>, HOLGER EBERHARDT<sup>1</sup>, DANIEL ELSNER<sup>1</sup>, ALESSIA FANTINI<sup>5</sup>, TORS- TEN FRESE<sup>1</sup>, FRANK FROMMBERGER<sup>1</sup>, VLADIMIR GANENKO<sup>4</sup>, GIAN- PIERO GERVINO<sup>6</sup>, FRANCESCO GHIO<sup>7</sup>, GIORGIO GIARDINA<sup>8</sup>, BRU- NO GIROLAMI<sup>7</sup>, DEREK GLAZIER<sup>9</sup>, STEFAN GOERTZ<sup>1</sup>, ANATO- LY GRIDNEV<sup>10</sup>, DANIEL HAHNE<sup>1</sup>, DANIEL HAMMANN<sup>1</sup>, JÜRGEN HANNAPPEL<sup>1</sup>, WOLFGANG HILLERT<sup>1</sup>, ALEXANDER IGNATOV<sup>11</sup>, FA- HIMEH JAHANBAKHSH<sup>2</sup>, OLIVER JAHN<sup>1</sup>, RAINER JAHN<sup>2</sup>, RUSSELL JOHNSTONE<sup>1</sup>, RAINER JOOSTEN<sup>2</sup>, TOM JUDE<sup>1</sup>, FRITZ KLEIN<sup>1</sup>, KAR- STEN KOOP<sup>2</sup>, BERND KRUSCHE<sup>12</sup>, ALEXANDER LAPIK<sup>11</sup>, PAOLO LEVI SANDRI<sup>7</sup>, IGOR LOPATIN<sup>10</sup>, GIUSEPPE MANDAGLIO<sup>8</sup>, FRAN- CESCO MESSI<sup>1</sup>, ROBERTO MESSI<sup>5</sup>, DARIO MORICCIANI<sup>5</sup>, VLADI- MIR NEDOREZOV<sup>11</sup>, DMITRY NOVISKIY<sup>10</sup>, PAOLO PEDRONI<sup>3</sup>, MARI- A ROMANIUK<sup>8</sup>, TIGRAN ROSTOMYAN<sup>12</sup>, CARLO SCHAEFER<sup>5</sup>, HART-

MUT SCHMIEDEN<sup>1</sup>, GEORG SIEBKE<sup>1</sup>, VICTORIN SUMACHEV<sup>10</sup>, VIA- CHESLAV TARAKANOV<sup>10</sup>, VALENTINA VEGNA<sup>1</sup>, PETR VLASOV<sup>2</sup>, DIE- TER WALTHER<sup>2</sup>, DAN WATTS<sup>9</sup>, HANS-GEORG ZAUNICK<sup>2</sup> und THO- MAS ZIMMERMANN<sup>1</sup> — <sup>1</sup>Physikalisches Institut, Nussallee 12, D-53115 Bonn — <sup>2</sup>Helmholtz-Institut für Strahlen und Kernphysik, Nussallee 14–16, D-53115 Bonn — <sup>3</sup>INFN sezione di Pavia, Via Agostino Bassi, 6 - 27100 Pavia Italy — <sup>4</sup>National Science Center Kharkov Institute of Physics and Technology, Akademicheskaya St. 1, Kharkov, 61108, Ukraine — <sup>5</sup>INFN Roma Tor Vergata, Via della Ricerca Scientifica 1, 00133 Rome - Italy — <sup>6</sup>INFN sezione di Torino, Via P.Giuria 1, 10125 Torino Italia — <sup>7</sup>INFN - LNF, Via E. Fermi 40, 00044 Frascati (Roma) Italy — <sup>8</sup>Università degli Studi di Messina, Via Consolato del Mare 41, 98121 Messina — <sup>9</sup>The University of Edinburgh, James Clerk Maxwell Building, Mayfield Road, Edinburgh EH9 3JZ UK — <sup>10</sup>Petersburg Nuclear Physics Institute, gatchina, Leningrad District, 188300 Russia — <sup>11</sup>Russian Academy of Sciences Institute for Nuclear Research, prospekt 60-letiya Oktyabrya 7a, Moscow 117312 Russia — <sup>12</sup>Institut für Physik, Klingelbergstrasse 82, CH-4056 Basel

**Участники от Лаборатории мезонной физики:**

**Д.Е. Баядилов, А.Б. Гриднев, И.В. Лопатин,**

**Д.В. Новинский, В.В. Сумачёв.**

## Introduction

Dedicated experimental programs exist to perform accurate measurements of meson photo- and electro-production off the nucleon in order to discover its excitations, and determine its internal structure. A new generation of electron accelerators equipped with tagged photon facilities have opened the way to meson photoproduction experiments of high sensitivity and precision [2]. The BGO-OD experiment at the ELSA facility at Bonn (see Figure 1) involves the use of a Bremsstrahlung tagged and polarized photon beam of energy between 0.7 and 3.2 GeV, a large solid angle high resolution BGO calorimeter and the Open Dipole spectrometer equipped with tracking detectors. This apparatus will be used to measure polarisation observables and cross sections in the photoproduction of pseudo-scalar and vector mesons off an hydrogen or deuterium target.

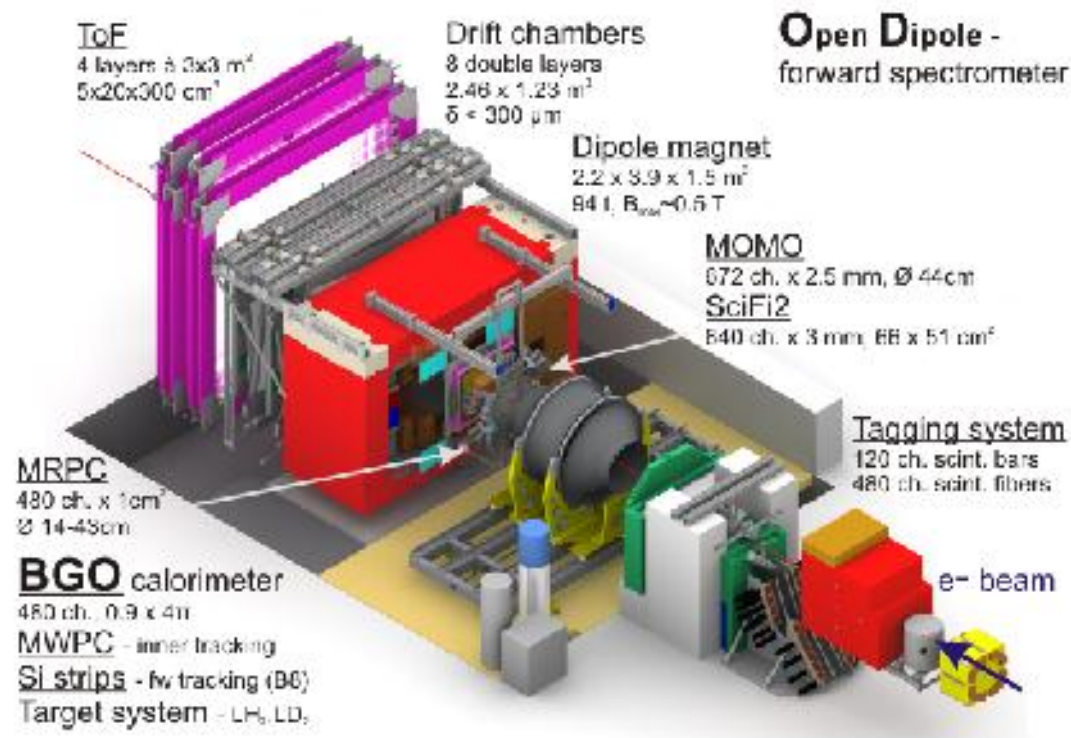


**Figure 2.** Schematic view of the Experimental Setup.

The BGO-OD detector setup is a combination of a central detector system and a forward spectrometer for charged particles, completed by a photon tagging system. The resolution of the tagger is about 1% ÷ 2% of the incident electron beam.

## The DC construction.

8 drift chambers are produced by PNPI according to agreement 153K-300-2/2007

( Detector Trackers №2 and №3 for B1 project. )

Configuration	Quantity
Horizontal sensitive wires ( X )	2 chambers
Vertical sensitive wires ( Y )	2 chambers
Inclined sensitive wires ( U, V )	4 chambers

DC sensitive area		
Horizontal area	2456	mm
Vertical area	1232	mm

To identify the detected particles, without the charged particle identification (the scintillator barrel was still not in operation during the beam time), the size of reconstructed clusters within the BGO was used. A cluster of three or more crystals was assumed to be a candidate photon, a cluster with only one crystal is a possible candidate proton or a charged pion [5].

Particularly, we observed that when the total energy deposit is below about  $300\text{ MeV}$  there is much low energy background to discern any structure in the spectrum. However above approximately  $400\text{ MeV}$  there is a concentration of events with the invariant mass close to the expected  $\pi^0$  mass, and a smaller shoulder above  $500\text{ MeV}$  is consistent with the mass of the  $\eta$  meson.

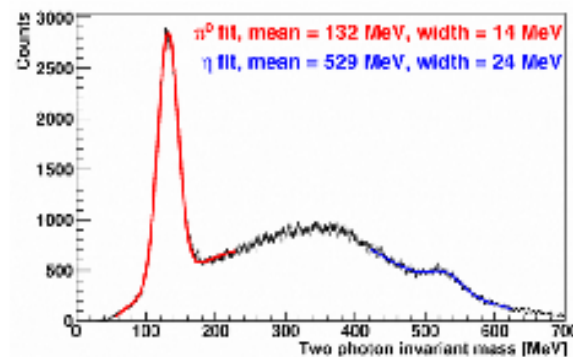


**Figure 9.** Two photon invariant mass spectrum taken with the BGO calorimeter in March 2012. [5, 6]



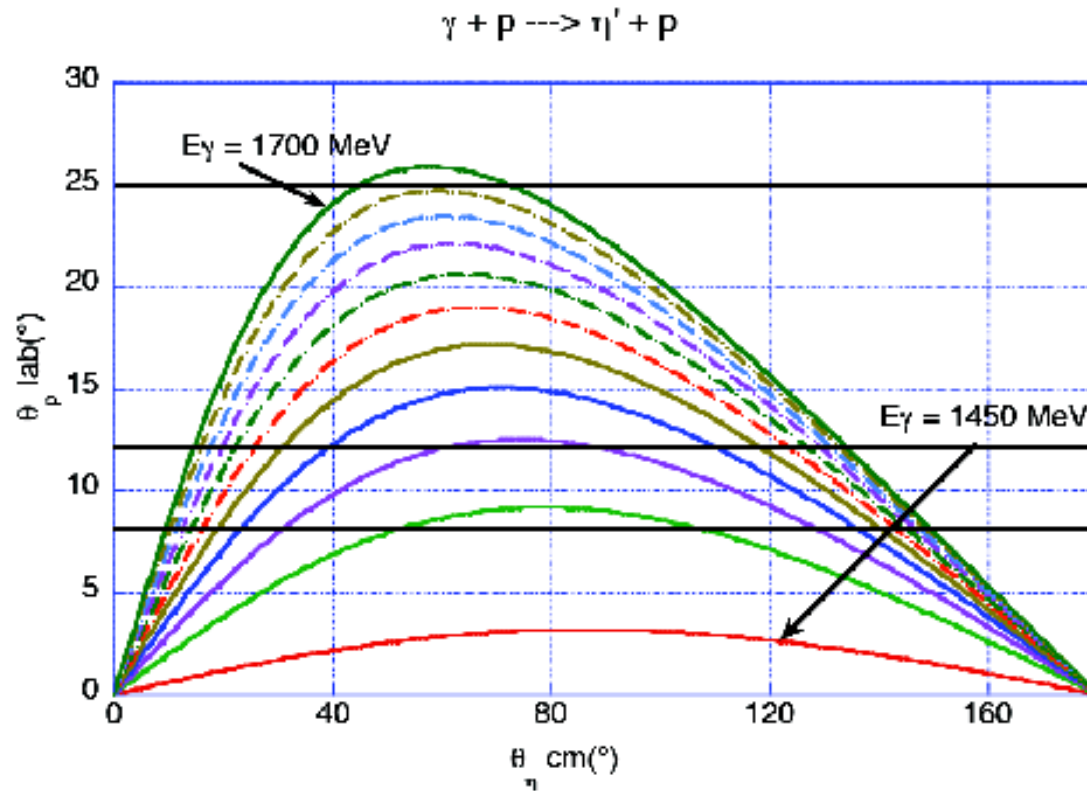


**Figure 10.** Kinematics of the reaction  $\gamma + p \rightarrow \eta' + p$ . The curves show (25 MeV steps for the incident photon energy  $E$ ) the behaviour of the proton laboratory angle  $\theta_p$  as a function of the  $\theta_{\eta'}$  center-of-mass angle.

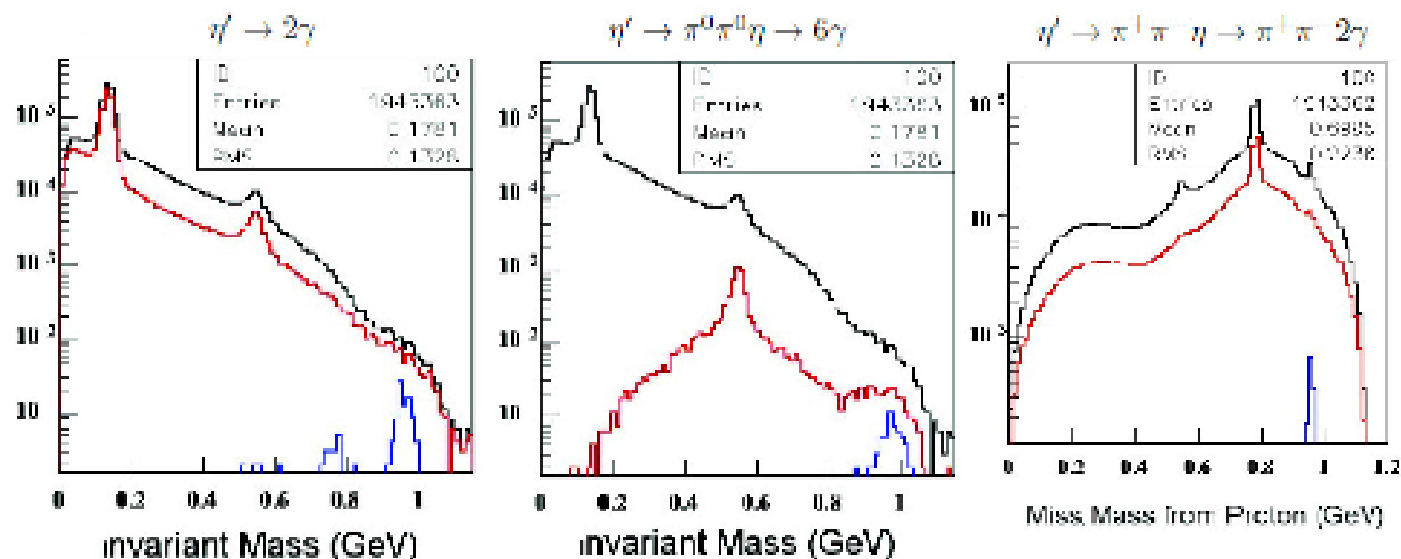


**Figure 11.** Event selection: the black curve is identical in left and central graphs and indicates the invariant mass spectrum of all events containing at least two photons measured in the BGO calorimeter, while in the right panel it indicates the missing mass from the detected forward proton. The red curve shows the same spectrum when exactly 2 photons(left), six photons(central), 2 photons and 2 identified charged pions (right) are reconstructed in the calorimeter. The blue curve shows the remaining events after the kinematical constraints from the recoil proton measurement are applied. In all cases (neutral and charged channels) the  $\eta$  peak is cleanly selected.

## Recent Results of the BGO-OD Experiment at ELSA Facility

### 6. Conclusions

During the February/March beam time 2012, for the first time, tests on totally equalized and calibrated BGO detector were performed with a full equipped BGO electronics consisting of 30 ADCs AVM-16 Mambo from Wiener. The calibrated energy and time of energy deposits in the BGO crystals have been used in the analysis. No charged particle identification was available (no data from the plastic scintillator barrel or MWPC) and no data from the photon tagger or any information from the forward spectrometer was used in the analysis. The reconstruction of the pseudoscalar mesons  $\eta$  and  $\pi^0$  from the decay photons was achieved. It was done plotting the two photon cluster invariant mass spectrum for events with at least 400 MeV energy deposit yields. It was performed an accurate feasibility study on the  $\gamma + p \rightarrow \eta' + p$  reaction, demonstrating the possibility to perform a  $\Sigma$  beam asymmetry measurement at BGO-OD experiment in the energy range starting from the threshold up to 1.7 GeV. We expect that the measure of this observable will be useful to contribute to solve the puzzle related to right weights of different resonances [8,9] involved in the reaction process, unsolved by the knowledge of the differential cross section [10–12].

## Project for B1 Collaboration

### “Bound states of the mesons and hyperons in the nuclei”

Gridnev A.B. Bayadilov D.E.

In a frame of B1 collaboration for the experiments with a beam of tagged photons with energies up to  $1500\text{ MeV}$ , PNPI scientific group proposed an experiment on investigation of bound states of  $\eta$ -meson with light nuclei.

Bound systems of strongly interacting particles have been extensively utilized to extract information about the various aspects of hadron-nucleon interaction. Familiar examples are studied of  $\Lambda N$  and  $\Sigma N$  interactions in a nuclear medium via analysis of the energy spectra of  $\Lambda$ - and  $\Sigma$ - hypernuclei. The strong attraction in  $\eta N$ - interaction was found in analysis [1, 2], leads to possible existence new type nuclei - bound state  $\eta$ - meson with nucleus ( $\eta$ - mesic nucleus) . The value of this attraction is depend on real part of the  $\eta N$ - scattering length. The reactions  $\pi^- p \rightarrow \eta n$  and  $\gamma p \rightarrow \eta p$  close to the threshold usually used to study  $\eta N$  interaction. However in ref. [3] was found that the real part of the  $\eta N$ - scattering length cannot be determined from cross sections of these reactions and a complicated multichannel should be used. This is the reason of large spread of the  $a_{\eta n}$  values reporting in different analysis (Table I)

Crystal Ball @ MAMI - Experiment

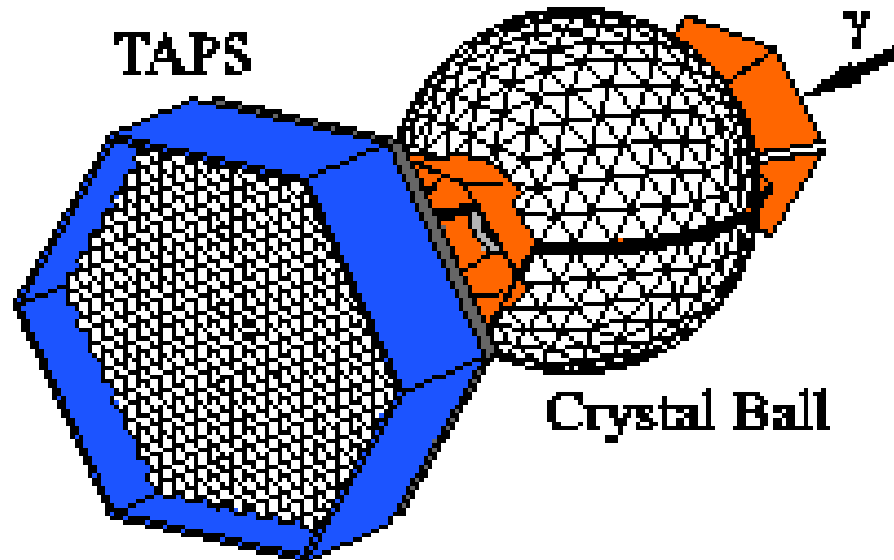


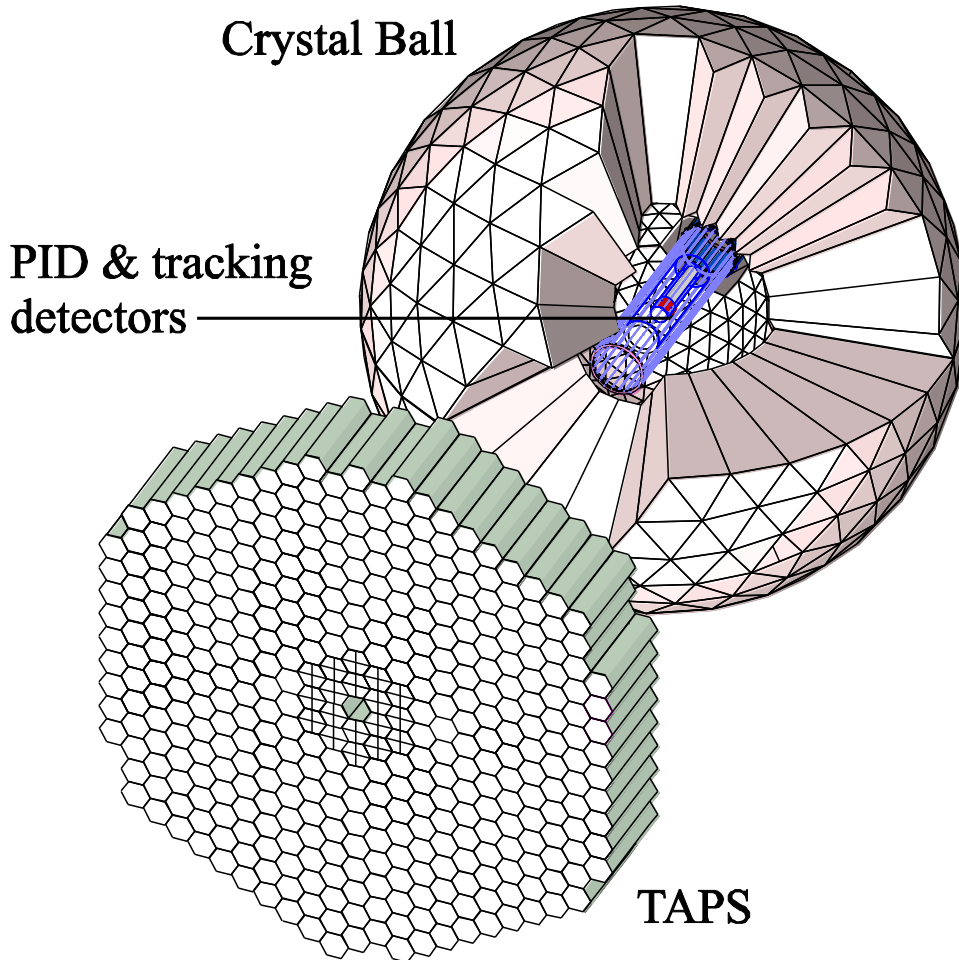
Fig. 1. The Crystal Ball/TAPS setup.

## Crystal Ball:

- $\mu^\pm$ : 233 MeV
- $\pi^\pm$ : 240 MeV
- $K^\pm$ : 341 MeV
- p: 425 MeV

## TAPS:

- $\mu^\pm$ : 165 MeV
- $\pi^\pm$ : 180 MeV
- $K^\pm$ : 280 MeV
- p: 360 MeV



## Crystal Ball:

- 672 NaI crystals about 16 *r.l.*
- Cover 94% solid angle
- Angular resolution:  $\sigma(\varphi)$  is 2-3 degree and
- $\sigma(\Theta)$  is  $(2^\circ-3^\circ)/\cos(\Theta)$
- Energy resolution of about  $\Delta E/E=0.02(E[\text{GeV}])-0.36$

## TAPS:

- 366 BaF2 and 72 PbWO crystals
- Time resolution 160 psec
- Overall acceptance for EC calorimeter 97%

## PID:

- Barrel of 24, 4 mm thick plastic strips
- Good time resolution
- Proton identification using  $\Delta E/\Delta x$

## MWPC:

- Two-layers cylindrical chamber
- Angular resolution 2-3 degrees
- Minimum material in particular in forward direction

## A narrow structure in the excitation function of $\eta$ -photoproduction off the neutron

(Dated: November 13, 2013)

The photoproduction of  $\eta$ -mesons off nucleons bound in  $^2\text{H}$  and  $^3\text{He}$  has been measured in coincidence with recoil protons and recoil neutrons for incident photon energies from threshold up to 1.4 GeV. The experiments were performed at the Mainz MAMI accelerator, using the Glasgow tagged photon facility. Decay photons from the  $\eta \rightarrow 2\gamma$  and  $\eta \rightarrow 3\pi^0$  decays and the recoil nucleons were detected with an almost  $4\pi$  electromagnetic calorimeter combining the Crystal Ball and TAPS detectors. The data from both targets are of excellent statistical quality and show a narrow structure in the excitation function of  $\gamma n \rightarrow n\eta$ . The results from the two measurements are consistent taking into account the expected effects from nuclear Fermi motion. The best estimates for position and intrinsic width of the structure are  $W = (1670 \pm 5)$  MeV and  $\Gamma = (30 \pm 15)$  MeV. For the first time precise results for the angular dependence of this structure have been extracted.

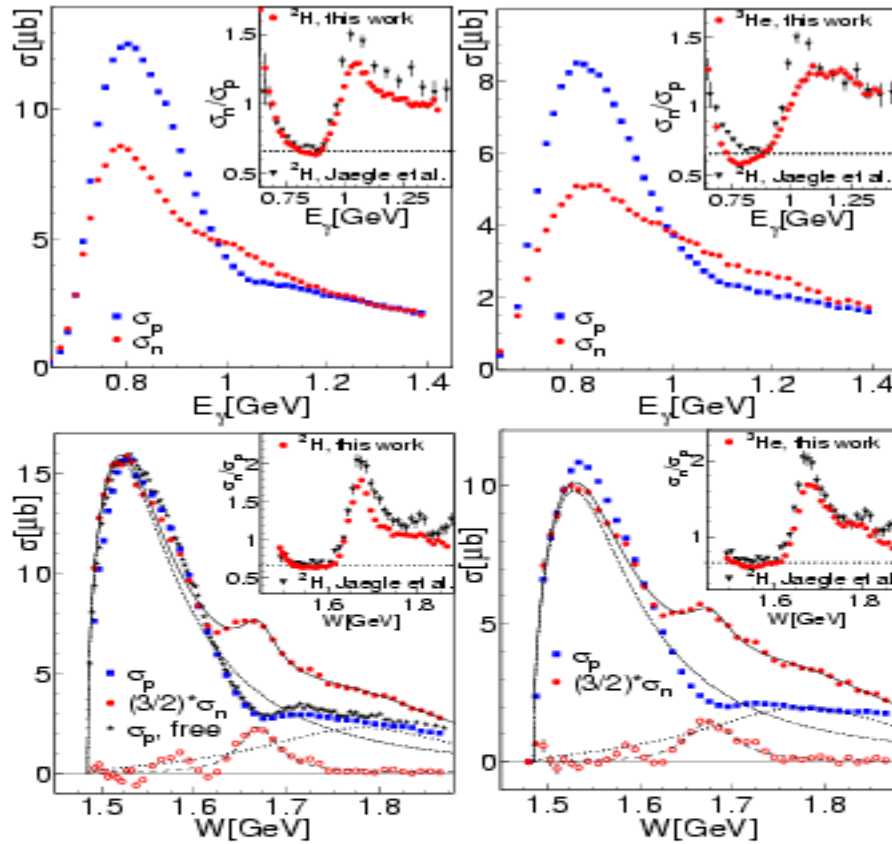


FIG. 1: Top: Total cross sections  $\sigma_p$  (coincident protons, blue squares) and  $\sigma_n$  (coincident neutrons, red circles) as function of incident photon energy  $E_\gamma$ . Left-hand side: deuterium target. Right-hand side: helium target. Bottom: same as function of reconstructed  $\eta N$  invariant mass  $W$ . Black stars: results for free proton [32]. The open red circles are present data after subtraction of the fitted  $S_{11}$  and background components. Curves: fit results for  $S_{11}$  resonance (dash-dotted), background (dotted), narrow structure (dashed), and full fit (solid). Insets for all figures:  $\sigma_n/\sigma_p$  ratio from present work (red circles) and from Ref. [6] (black triangles).



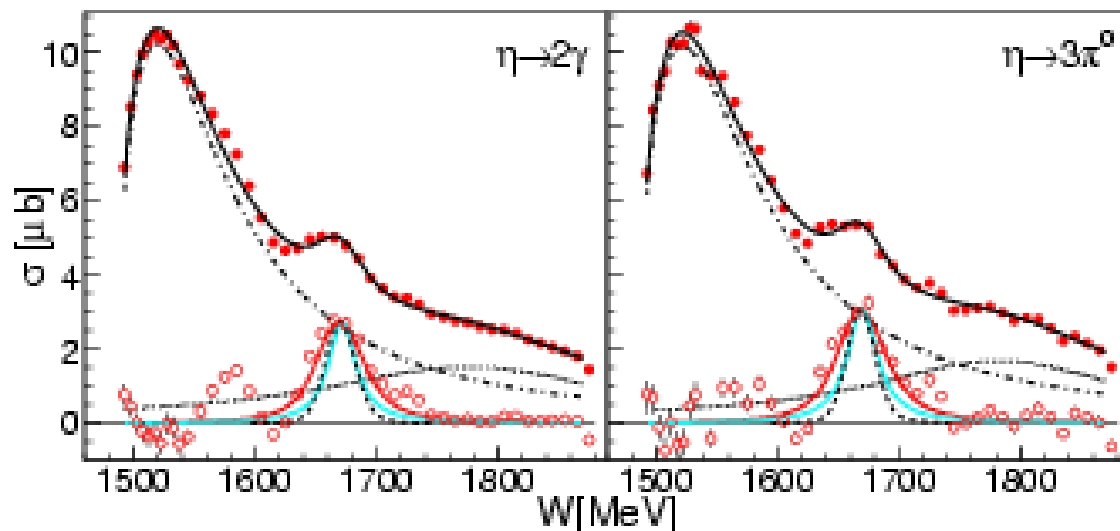


FIG. 2: Excitation functions for  $\gamma n \rightarrow n\eta$  from the deuteron target. Left-hand side from  $\eta \rightarrow 2\gamma$  decay, right-hand side from  $\eta \rightarrow 3\pi^0$  decay. Solid curve and dashed curves: fit components like in Fig. 1. Open symbols: data with background fit subtracted (scaled up by factor of 2). Curves at bottom: experimental resolution dashed (black), fitted signal (red), intrinsic signal shape (light blue) (see text).

## Measurement of the ${}^1H(\vec{\gamma}, \vec{p})\pi^0$ reaction using a novel nucleon spin polarimeter

(Dated: October 1, 2013)

We report the first large-acceptance measurement of polarization transfer from a polarized photon beam to a recoiling nucleon, pioneering a novel polarimetry technique with wide application to future nuclear and hadronic physics experiments. The commissioning measurement of polarization transfer in the  ${}^1H(\vec{\gamma}, \vec{p})\pi^0$  reaction in the range  $0.4 < E_\gamma < 1.4$  GeV is highly selective regarding the basic parameterizations used in partial wave analyses to extract the nucleon excitation spectrum. The new data strongly favor the recently proposed Chew-Mandelstam formalism.

PACS numbers: 13.60.La, 24.85.+p, 25.10.+s, 25.20.-x

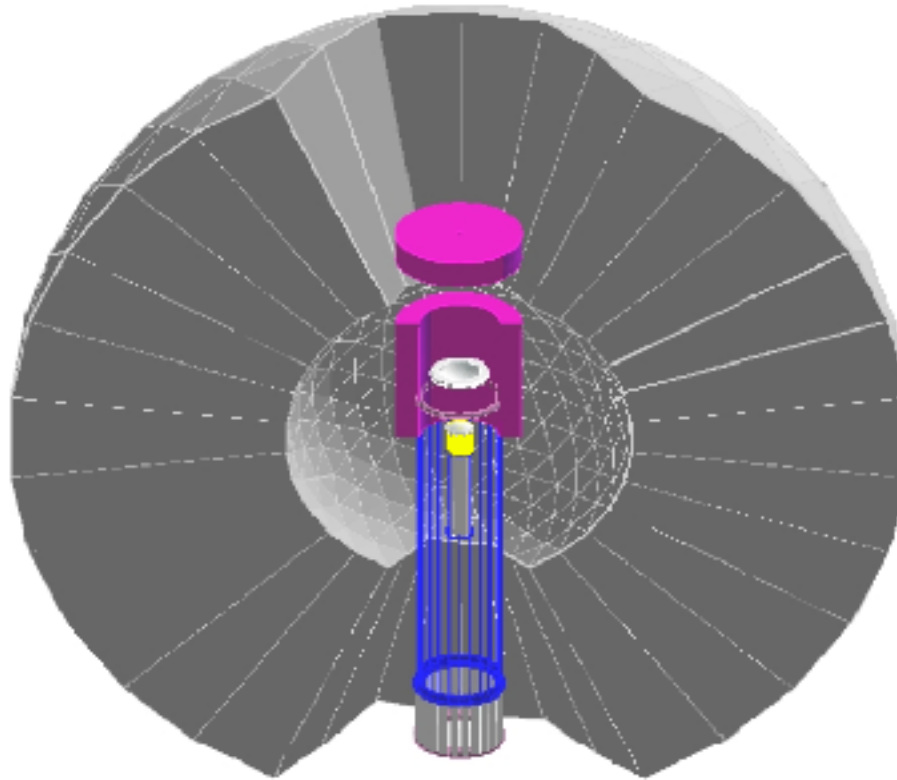


FIG. 1: (Color online) Illustration of the experimental setup. The liquid hydrogen target (yellow cylinder), situated at the center of the CB, is surrounded by the PID (blue) and the 2.25 cm thick graphite polarimeter. The 7.25 cm thick upstream cap covers the upstream aperture to TAPS (not pictured). The PID was flush with the upstream cap during data acquisition, however for this picture, the PID has been shifted for clarity.

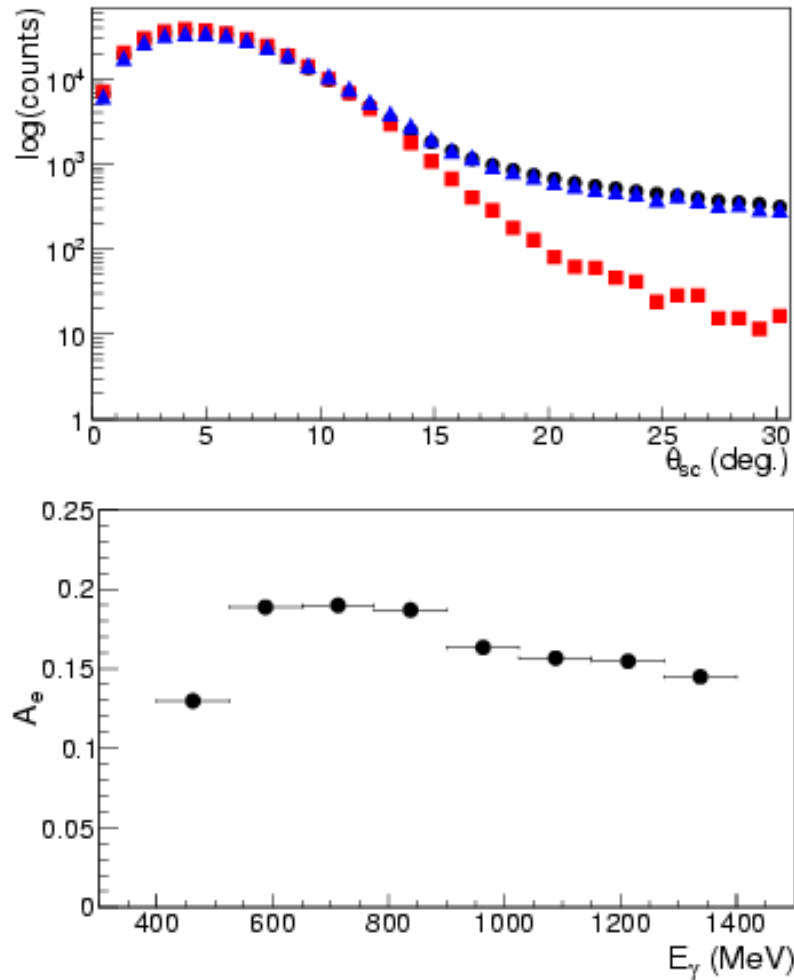


FIG. 2: (Color online) (Top) Comparison of  $\theta_{sc}$  for data (circles), simulation (triangles), and the simulation with no hadronic interaction (squares). Nuclear scattered events lie in the shaded region. (Bottom) The average of the effective analyzing powers obtained from each model, integrated over  $\theta_{CM}$ . The shaded region indicates the systematic error.

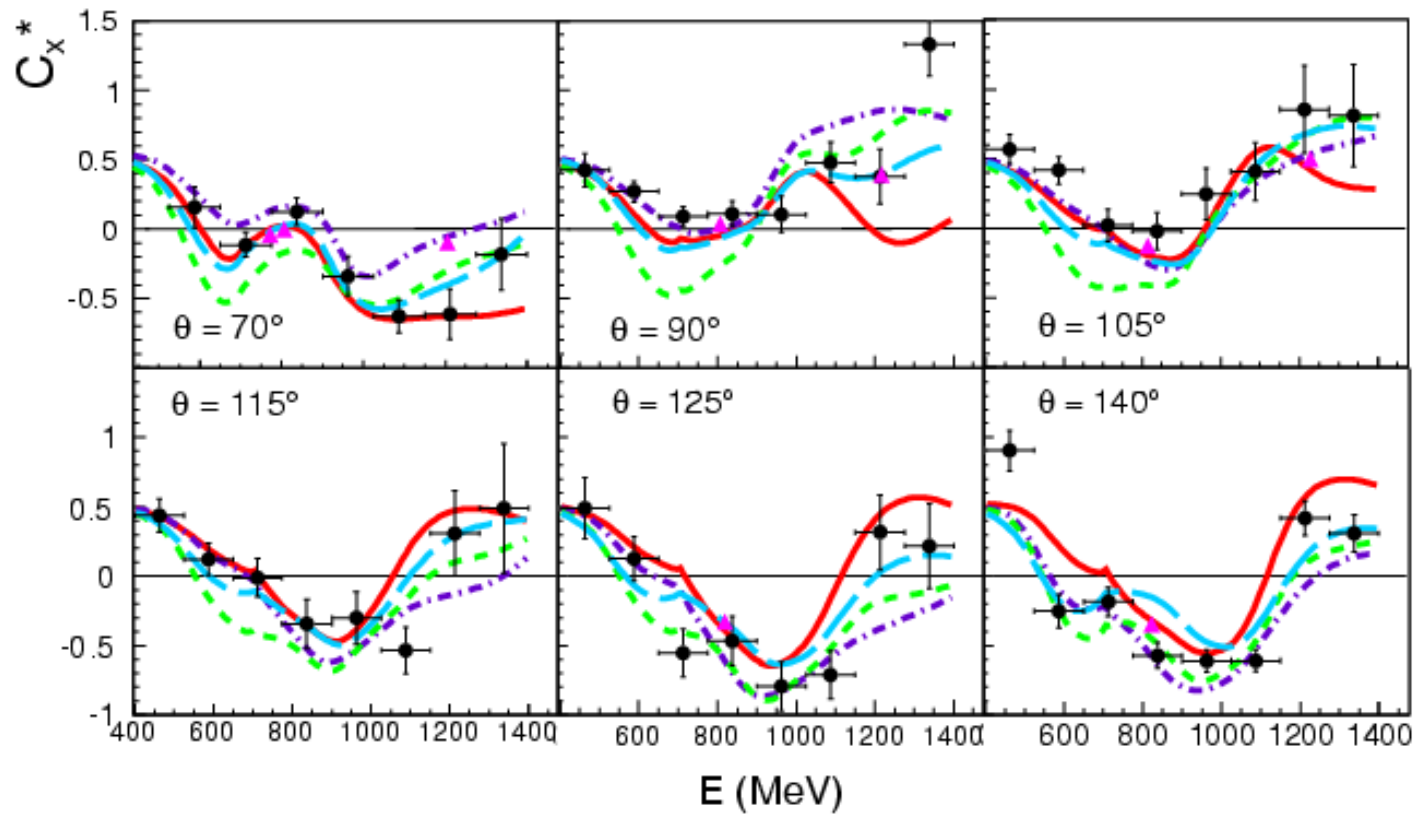


FIG. 3: (Color online)  $C_x^*$  excitation functions for  $\vec{\gamma}p \rightarrow \pi^0 \vec{p}$  (black circles) for fixed pion CM polar angles. Previous data came from JLab Hall A [3] (magenta triangles). The PWA solutions shown are: SAID CM12 [33] (cyan long-dash line), SAID SN11 [34] (green short-dash line), BnGa2011-2 [35] (solid red line), and MAID07 [36] (violet dash-dotted line).

## Measurement of the $^1H(\vec{\gamma}, \vec{p})\pi^0$ reaction using a novel nucleon spin polarimeter

### IV. SUMMARY AND CONCLUSION

A new polarimeter concept has been developed to determine the spin of the proton produced in nuclear and hadronic reactions with large acceptance and kinematic coverage. This novel, cost effective method for large acceptance spin-polarimetry could also find application at many other facilities with large acceptance particle detectors such as ELSA, JLab, and FAIR where new possibilities for spin observable measurements in meson spectroscopy, baryon spectroscopy and nuclear structure physics are possible.

In the commissioning experiment a comprehensive set of data for the transfer of polarization to the recoiling nucleon ( $C_x^*$ ) was obtained for neutral-pion photoproduction on the proton at incident photon energies from 0.4 to 1.4 GeV using the MAMI-C tagged-photon beam. The data are a central piece of the ongoing nucleon resonance program and give strong evidence that the Chew-Mandelstam formalism should be used if reliable information on the excitation spectrum is to be obtained.

# ЛМФ 2013 (Гамма-физика)

Veronica De Leo, B Bantes, <u>D Bayadilov</u> ,	Recent results of the BGO-OD experiment at ELSA facility. 12 pp.	J.Phys.Conf.Ser. 424 (2013) 012008
A.V. Anisovich, E. Klempt, <u>V. Kuznetsov</u> , V.A. Nikonov, M.V. Polyakov, A.V. Sarantsev, U. Thoma.	Study of the narrow structure at 1685-MeV in gamma p ---> eta p.	Phys.Lett. B719 (2013) 89-94, 6 pp.
..., V.Bekrenev,...	Double pion photoproduction off nuclei - are there effects beyond Final State Interaction.	Phys.Lett. B722 (2013) 69-75.
P. Aguar Bartolome, A. Mushkarenkov, J. Ahrens, J.R.M. Annand, R. Beck, <u>V. Bekrenev</u> , H. Berghäuser, A. Braghieri,	First measurement of the helicity dependence of $^3\text{He}$ photoreactions in the $\Delta(1232)$ resonance region.	Phys.Lett.B723(2013)71-77
...V.Bekrenev,...A.Kulbardis ,S.P.Kruglov,...	Measurements of $^{12}\text{C}(\gamma,pp)$ photon asymmetries for $E_{\gamma}=200-450$ MeV.	EPJA 49 (2013) 65
M. Oberle, ... <u>V. Bekrenev</u> , ... <u>S.P. Kruglov</u> , <u>A. Kulbardis</u> et al.	Measurement of the beam-helicity asymmetry $S_{1}^{\odot}$ in the photoproduction of $\pi^0$ -pairs off the proton and off the neutron.	Phys.Lett.B 721 (2013) 237-243.

Crystal Ball Collaboration	Coherent photoproduction of $\pi^0$ - and $\eta$ -mesons off $^7\text{Li}$ .	Eur.Phys.J. A49 (2013) 38
M. Thiel, V. Metag, P. Aguar Bartolome, L.K. Akasoy, J.R.M. Annand, H.J. Arends, V. Bekrenev, ... <u>A. Kulbardis</u> et al.	In-medium modifications of the $\omega$ meson near the production threshold.	Eur.Phys.J. A49 (2013) 132 (2013)
A2 and CB-TAPS Collaboration (D. Hornidge, P. Aguar Bartolome, J , R. Beck, <u>V. Bekrenev</u> , ... <u>A. Koulbardis</u> , D. Krambrich, <u>S. Kruglov</u> et al. )	Accurate Test of Chiral Dynamics in the $\gamma \rightarrow \pi^0 p$ Reaction	Phys.Rev.Lett. 111 (2013) 062004
M.Gottschall, A.V. Anisovich, B. Bantes, <u>D. Bayadilov</u> , ... <u>I. Lopatin</u> ,... <u>V. Sumachev</u> at all. (The CBELSA/TAPS Collaboration).	First measurement of the helicity asymmetry for $\gamma p \rightarrow \rho\pi^0$ in the resonance region	ArXiv:1312.2187 [nucl-ex]
M. Nanova, V. Metag, ... <u>D. Bayadilov</u> ,.R. Beck, .. <u>Yu.A.Beloglazov</u> , .. <u>A. B. Gridnev</u> ,.... <u>I.V. Lopatin</u> , at all (The CBELSA/TAPS Collaboration).	Determination of the $\eta'$ -nucleus optical potential	Physics Letters B 727 (2013), pp. 417-423



Поиск узких резонансов в неупругих каналах  $\pi$ -р-рассеяния  
56-я научная конференция МФТИ, г. Долгопрудный, Россия,  
25-30 ноября 2013 года, 1230 участников.

Прецизионный безмагнитный спектрометр для эксперимента ЭПЕКУР  
56-я научная конференция МФТИ, г. Долгопрудный,  
Россия, 25-30 ноября 2013 года, 1230 участников.

New results on narrow structure in the pion nucleon elastic scattering  
from the EPECUR experiment  
XV International Conference on Hadron Spectroscopy (Hadron 2013)  
November 4th to November 8th 2013 Nara, Japan.

Experiment EPECUR for High Precision Measurements of the Pion Proton Cross Section  
in the Second Resonance Region  
XV International Conference on Hadron Spectroscopy (Hadron 2013)  
November 4th to November 8th 2013 Nara, Japan.

New generation data on  $\pi p$ -elastic cross section from the EPECUR experiment  
BARYONS 2013, University of Glasgow, Scotland, June 24–28, 2013.

High precision measurements of the pion-proton elastic differential elastic cross section  
in the second resonance region  
NSTAR 2013 Workshop Peñíscola, Valencian Community (Spain), May 27-30, 2013.